Vol 17 No 9, September 2008
1674-1056/2008/17(09)/3516-07

Chinese Physics B

© 2008 Chin. Phys. Soc.
and IOP Publishing Ltd

Phase field simulation of the columnar dendritic growth and microsegregation in a binary alloy*

Li Jun-Jie(李俊杰), Wang Jin-Cheng(王锦程)†, and Yang Gen-Cang(杨根仓)

State Key Laboratory of Solidification Processing, Northwestern Polytechnical University, Xi'an 710072, *China*

(Received 23 January 2008; revised manuscript received 24 February 2008)

This paper applies a phase field model for polycrystalline solidification in binary alloys to simulate the formation and growth of the columnar dendritic array under the isothermal and constant cooling conditions. The solidification process and microsegregation in the mushy zone are analysed in detail. It is shown that under the isothermal condition solidification will stop after the formation of the mushy zone, but dendritic coarsening will progress continuously, which results in the decrease of the total interface area. Under the constant cooling condition the mushy zone will solidify and coarsen simultaneously. For the constant cooling solidification, microsegregation predicted by a modified Brody-Flemings model is compared with the simulation results. It is found that the Fourier number which characterizes microsegregation is different for regions with different microstructures. Dendritic coarsening and the larger area of interface should account for the enhanced Fourier number in the region with well developed second dendritic arms.

Keywords: phase field model, solidification, columnar dendrite, microsegregation
PACC: 8130F, 6475, 7115Q

1. Introduction

The formation of complex solidification patterns is a typical nonequilibrium phenomenon and represents a conceptually simple example of self-organization. Consisting of both the columnar and equiaxed dendrites，dendritic structures are prevalent in most cast alloys and play an essential role in determining the final quality of casting products. In addition, microsegregation within dendritic structures also has great influences on the performance of products. Therefore, the descriptions of dendritic structures and microsegregation are key steps towards a complete understanding and controlling of solidification process.

Many analytical models of microsegregation have been proposed and extended[1−6] to calculate the chemical inhomogeneity at the scale of dendritic arms, but in all these models some simplifications of dendritic morphology were assumed. In principle, the microsegregation has a close relationship with the microstructure. Yan *et al*[7] showed that using different geometrical models to approximate the shape of dendrite would give different microsegregation patterns. So the proper description of dendritic morphology is important in modelling microsegregation. The phase field method has been successfully employed as a powerful tool for describing complex solidification structures.[8−11] In the phase field simulation the evolution of the microstructure and concentration field can be explicitly tracked in a physical manner, which results in the convenience to analyse the microsegregation. In this paper a phase field model for polycrystalline solidification is applied to simulate the formation and growth of columnar dendritic array. The concentration distribution within dendritic array is analysed and compared with the classical microsegregation models.

2. Phase field model

Based on the work of Kim *et al*,[12] Kobayashi *et al* [13] and Gránásy *et al*,[14] we have developed a phase field model for polycrystalline solidification in binary alloys.[15] Evolution of the phase field, orientation field and concentration field are described by

$$\begin{aligned}\frac{1}{M_\phi}\frac{\partial\phi}{\partial t} =&\nabla(\varepsilon^2\nabla\phi) - Hh'(\phi)\,|\nabla\theta| - wg'(\phi)\\ &+ h'(\phi)[f^{\mathrm{L}}(c_{\mathrm{L}}) - f^{\mathrm{S}}(c_{\mathrm{S}}) - (c_{\mathrm{L}}\\ &- c_{\mathrm{S}})f^{\mathrm{L}}_{c_{\mathrm{L}}}(c_{\mathrm{L}})],\end{aligned} \tag{1}$$

*Project supported by the National Natural Science Foundation of China (Grant No 50401013) and Doctorate Foundation of Northwestern Polytechnical University, China.
†E-mail: jchwang@nwpu.edu.cn

$$\frac{1}{M_\theta}\frac{\partial\theta}{\partial t} = H\nabla\left[h(\phi)\frac{\nabla\theta}{|\nabla\theta|}\right], \quad (2)$$

$$\frac{\partial c}{\partial t} = \nabla[D(\phi)\nabla c] + \nabla[D(\phi)h'(\phi)(c_{\rm L} - c_{\rm S})\nabla\phi], \quad (3)$$

where $f^{\rm S}(c_{\rm S})$ and $f^{\rm L}(c_{\rm L})$ are the free energy densities of the solid and liquid phase respectively, $h(\phi) = \phi^2(3-2\phi)$, $g(\phi) = \phi^2(1-\phi)^2$. The solute diffusivity is defined as $D(\phi) = D_{\rm S}h(\phi)+(1-h(\phi))D_{\rm L}$, $D_{\rm S}$ and $D_{\rm L}$ are the diffusion coefficient in the solid and liquid respectively. c is determined to be the fraction-weighted average value of the solid concentration $c_{\rm S}$ and the liquid concentration $c_{\rm L}$, $c = h(\phi)c_{\rm S} + [1 - h(\phi)]c_{\rm L}$. In the interface region the chemical potentials of solid $f^{\rm S}_{c_{\rm S}}[c_{\rm S}(x,t)]$ and liquid $f^{\rm L}_{c_{\rm L}}[c_{\rm L}(x,t)]$ are assumed to be equal. See Ref.[15] for more details about this model.

During the phase field calculation, an uniform distributed stochastic noise term (the amplitude is 0.01) is added at the interface in order to simulate the fluctuations, which results in the well developed secondary arms.

3. Results and discussion

Solidification processes of the Ni–0.396mol%Cu alloy under isothermal and constant cooling conditions are simulated. The material parameters are as follows: diffusion coefficients $D_{\rm S} = 1 \times 10^{-12}{\rm m}^2/{\rm s}$, $D_{\rm L} = 1 \times 10^{-9}{\rm m}^2/{\rm s}$, interface energy $\sigma = 0.35$ J/m^2, molar volume $V_{\rm m} = 7.42\times10^{-6}$ m^3/mol, partition coefficient k=0.87, magnitude of anisotropy $r = 0.04$, mesh size $\Delta x = \Delta y = 5.0 \times 10^{-8}$m, the computational domain size is 2000×2000 in terms of grid number. The temperature of the system is assumed to be uniform in both the isothermal and constant cooling conditions. In the former case the temperature is set to be 1576K for all the time, while in the latter case it will decrease from 1580 K with a constant cooling rate of 75 K/s. As an initial condition, twenty nuclei are set at the left side of the domain, and they will grow into the undercooled melts.

3.1. Dendritic growth under the isothermal condition

The evolution of solidification structure in the isothermal case is shown in Fig.1. The solidification starts at the left side boundary, then the initial grains impinge with each other as they have different crystallographic orientations. The dendrites extend faster into the bulk liquid when their < 001 > crystallographic orientation is perpendicular to the left side boundary, and the growth in other directions is suppressed. Therefore a columnar dendritic structure forms. This selection mechanism in the system with an uniform temperature is not really based on a minimum undercooling criterion, but rather on a 'minimum travel' criterion as pointed out by Rappaz and Gandin.[16]

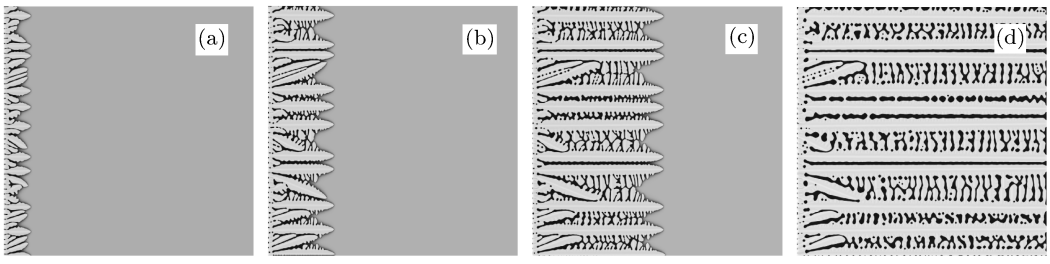


Fig.1. Simulated microstructural during isothermal solidification at 1576 K after: (a) 5 ms, (b) 12.5 ms, (c) 25 ms, and (d) 87.5 ms.

Figure 2 illustrates the variation of the average concentrations in the liquid $c_{\rm L}$ and solid $c_{\rm S}$ with x at different times, and the schematic representation of three regions divided according to the change of $c_{\rm L}$. The values of $c_{\rm L}$ and $c_{\rm S}$ are obtained by averaging the calculated concentrations separately in the liquid and solid along the grid line in y direction. It can be found that, in the region I, the side branches are well developed and the spacing of dendritic arms are relatively small, and the average liquid concentration approximately keeps constant in this region. Here we call this region the mushy zone. In region III, called as liquid zone, there is no solid phase and the average liquid concentration holds the initial value because the so-

lute diffusion length of dendrites is small. The region II is called as dendritic tip zone, where the value of average liquid concentration gradually changes from the one in mushy zone to that in liquid zone. For the temperature is set to be constant in this case, the solidification in the mushy zone will stop, and the average concentrations of liquid and solid will approximately keep constant as shown in Fig.2(a).

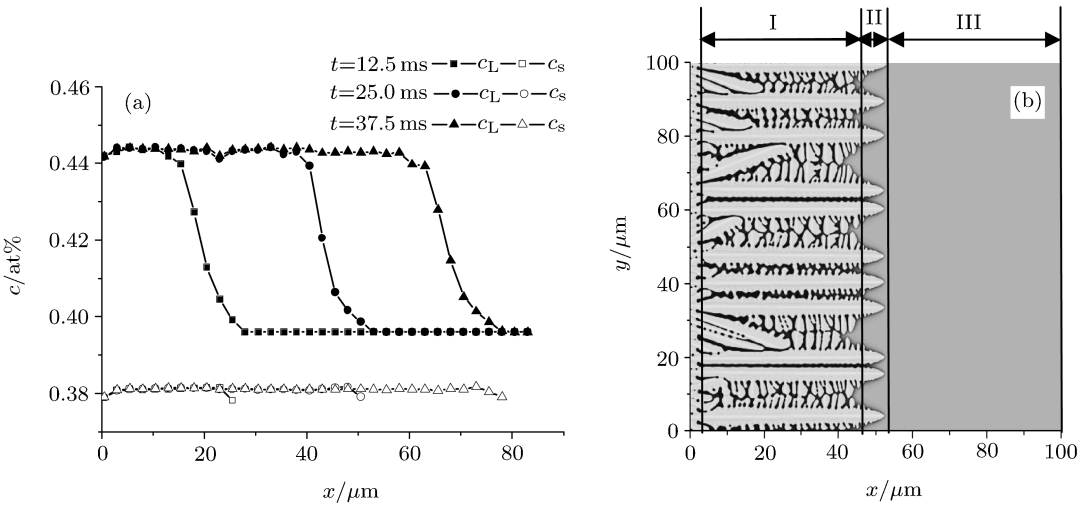


Fig.2. (a) Variations of the average concentrations in the liquid c_{L} and solid c_{S} with distance x at different times under isothermal condition, and (b) the schematic representation of three regions divided according to the change of c_{L}.

Coarsening of dentritic arm is a surface tension driven phenomenon, during which the secondary dendritic arm spacing and the total surface area will decrease. Under isothermal conditions, although the solidification in the mushy zone stops, the coarsening of dendritic arms progresses after the solidification, which can be reflected by exploring the variation of total surface area (Fig.3) and the distribution of liquid concentration (Fig.4). As shown in Fig.3, after the dendrites reach the right boundary of the system, the solid fraction of the whole system will keep constant, while fraction of total interface will decrease due to the dendritic coarsening. Figure 4(a) is the concentration the histogram for the area that x changes from $30\,\mu$m to $40\,\mu$m at two different times. The two peaks with increasing levels of concentration correspond to solid and interdendritic liquid. The interdendritic liquid peak contains a spread in composition reflecting the positive and negative curvatures of the interface between the liquid and solid. With the coarsening of dendritic arms the interface curvature will be uniform and the high curvature part will disappear, so the interdendritic liquid concentration will become uniform, which can be reflected by the sharpening of the interdendritic liquid peak (see the enlarged graph in Fig.4(a)).

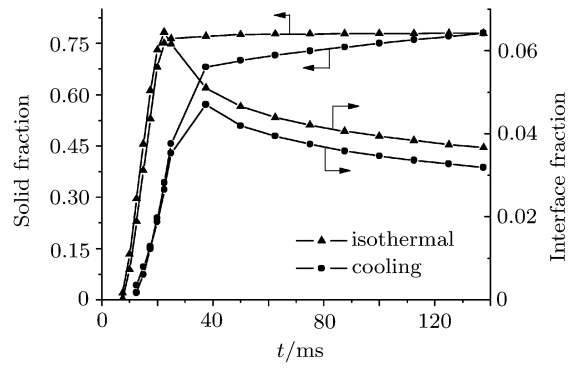


Fig.3. The fractions of solid and interface against solidification time under isothermal and constant cooling conditions.

3.2. Dendritic growth under the constant cooling condition

The microstructure evolution under the constant cooling condition is similar to that under the isothermal condition. However the concentration distribution is quite different as shown in Fig.5. The average concentration of solid varies along the x direction and increases with the time as the temperature decreases continuously. Due to the high diffusivity in the liquid, the average concentration of liquid in the mushy zone approximately keeps uniform, but will increase with time. The increases of average concentrations of liquid

and solid in the mushy zone with time indicate the successive solidification in this region after its formation. This can be also observed from the variation of solid fraction with time in Fig.3. The initial quick raise of the solid fraction curve corresponds to the growth of dendrites into the undercooled liquid, and then the following gentle increase indicates the solidification in the mushy zone, which accompanies with the decrease of interface area arising from the dendritic coarsening. The coarsening can also be found from analysing the concentration histogram for the area that x changes from 30 μm to 40 μm at two different times (Fig.4(b)). Other than the increase of the concentration of solid and interdendritic liquid due to the solidification of the mushy zone, the regularity of Fig.4(b) is similar to that of Fig.4(a).

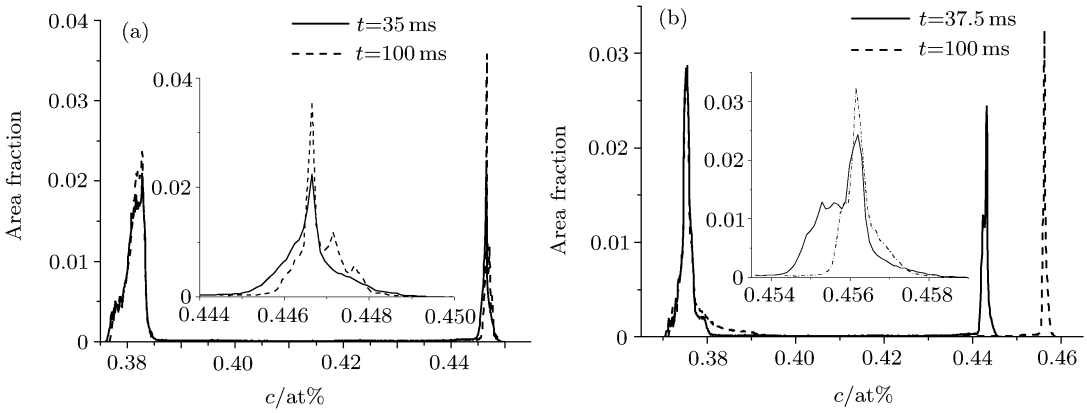


Fig.4. Histograms of the fraction of area vs concentration at different times in the region that x changes from 30 μm to 40 μm, under (a) isothermal condition, (b) constant cooling condition. The insert is an enlarged part of the peak in the liquid phase, the data for the insert in (b) have been shifted for better presentation.

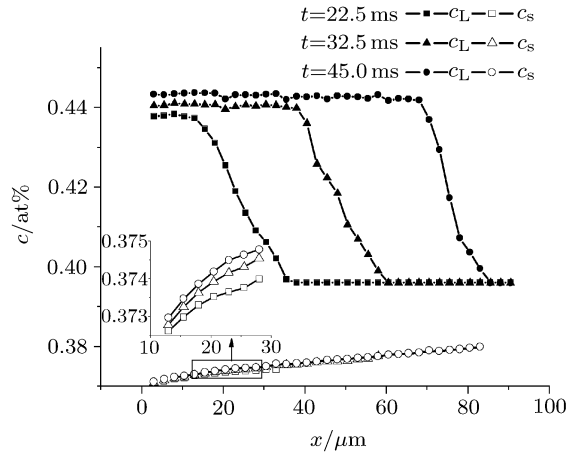


Fig.5. Variations of the average concentrations in the liquid and solid with x at different times under constant cooling condition.

3.3. Microsegregation within dendritic array under the constant cooling condition

Just as shown in Figs.2 and 5, there is a large liquid concentration variety in the dendritic tip zone, which disobeys the assumption made by most analytical microsegregation models, *i.e.*, complete mixing of liquid. Only after the formation of mushy zone, the liquid concentration can be approximately uniform. In addition, it should be noted that the high initial undercooling and cooling rate in our simulation will lead to nonequilibrium solidification. This will also make the simulation results deviate from analytical microsegregation models. However our analyses indicate that nonequilibrium solidification only happens during the initial stage of dendritic tip growth, but not in the whole process. The evolution of the total undercooling as a function of solid fraction for region A (the area with x changing from 5 μm to 15 μm) and region B (the area with x changing from 50 μm to 65 μm) are shown in Fig.6. It can be seen that at the beginning of solidification there is a high undercooling. So nonequilibrium solidification occurs at this stage. With the progress of solidification the solute constituents are rejected into the liquid phase. When the volume fraction of solid is high, which means that the mushy zone has formed, the undercooling in regions A and B will become very low. So the solidification in the mushy zone is near equilibrium.

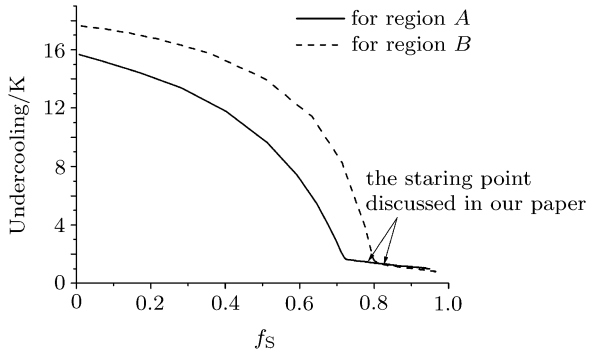


Fig.6. The undercooling evolution as a function of the solid fraction.

Based on the above analyses, in order to compare simulation results with analytical microsegregation models, we only study the near equilibrium solidification after the formation of mushy zone under the constant cooling condition. One issue pointed by Giovanola and Kurz[5] should be noted, i.e., in this situation the initial state should be $c_L = c_x$ at $f_S = f_x$ (instead of $c_L = c_0$ at $f_S = 0$ in the case of standard microsegregation equation), where the value of c_x and f_x can be chosen at any time after the complete mixing of liquid. After taking this point into account, the standard Scheil equation, lever rule and Brody–Flemings model can be modified as:

$$c_L = c_x \left(\frac{1 - f_S}{1 - f_x} \right)^{k-1}, \tag{4}$$

$$c_L = c_x \frac{1 - (1-k) f_x}{1 - (1-k) f_S}, \tag{5}$$

$$c_L = c_x \left[\frac{1 - (1 - 2\alpha k) f_S}{1 - (1 - 2\alpha k) f_x} \right]^{\frac{k-1}{1-2\alpha k}}, \tag{6}$$

where k is the partition coefficient, α is the Fourier number, which characterizes the solid-state diffusion (so called back diffusion). The derivation of equations (4)–(6) is given in the Appendix. Some modifications have been proposed to get more exact solutions[2−4] to the back diffusion problem. What we concerned here is the different extents of back diffusion in regions with different microstructures. So we will take α as a fitting parameter and not use the more sophisticated back diffusion models.[2−4]

Microsegregation within regions A and B is invested. The microstructure evolutions in regions A and B are shown in Fig.7. It can be seen that the second dendritic arms are well developed in region B, whereas there are only slick primary arms in region A. Microsegregation forming at the stage of mushy zone solidification is shown in Fig.8. It can be found that the simulation results lie between the Scheil equation and lever rule just as expected, and with properly choosing parameter, α=0.0257 for region A and α=0.0685 for region B, the Brody–Flemings model can agree well with the simulation results. Compared with region A, the increase of Fourier number for region B means an enhanced back diffusion in this region. The solid diffusion coefficient is the same in the two regions, so the enhanced back diffusion should be attributed to their different microstructures. The coarsening of second dendritic arms in region B leads to an increase of arm spacing. This effect equals to increasing the Fourier number just as pointed by Voller and Beckermann.[6] Furthermore, well developed dendrite arms lead to a larger area of solid/liquid interface per unit volume. The amount of solute transferred by solid diffusion is proportional to the interface area. So the effect of back diffusion is pronounced in region B.

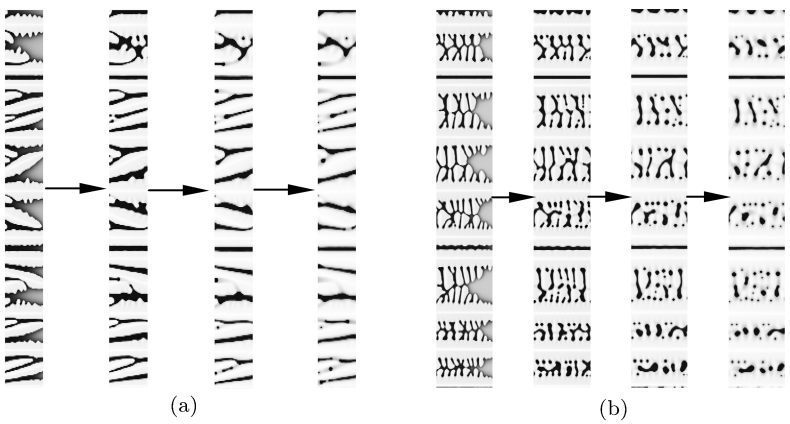


Fig.7. Simulated microstructure evolution for region A (a) and region B (b).

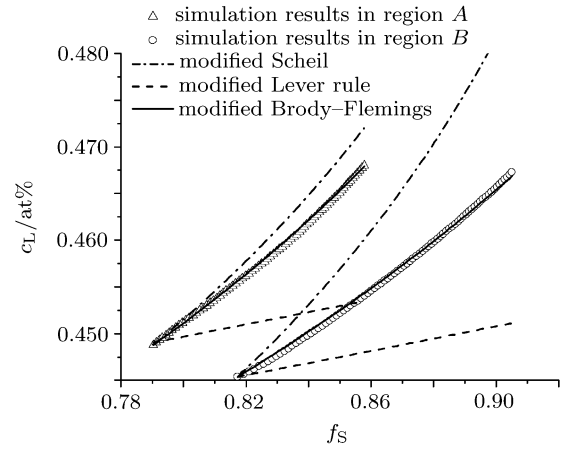


Fig.8. Liquid concentration profiles as a function of the solid fraction for the solidification of mushy zone.

4. Conclusions

Polycrystalline solidifications in Ni–0.396mol%Cu alloy under isothermal and constant cooling conditions are simulated by using the phase field method. The transition from initial equiaxed grains to the columnar dendritic array based on the 'minimum travel' criterion proposed by Rappaz and Gandin[16] is well reproduced by the phase field simulation. Under the isothermal condition solidification will stop after the formation of the mushy zone, but dendritic coarsening will progress continuously, which results in the decrease of the total interface area. Under the constant cooling condition the mushy zone will solidify and coarsen simultaneously. The simulation results of microsegregation agree with the modified Brody–Flemings model. It is also found that the Fourier number which characterizes microsegregation is different for regions with and without well developed second dendritic arms. Dendritic coarsening and the larger area of interface should account for the enhanced Fourier number in the region with well developed second dendritic arms.

Appendix

We consider a small volume element in the mushy zone and approximate the solidification by the planar geometry as shown in Fig.A1. Microsegregation models base on the following assumptions:

(1) diffusion in the liquid is complete, i.e., at any point in time the solute concentration in the liquid phase c_L is uniform;

(2) equilibrium is maintained at the solid–liquid interface, i.e., $c_S^i = kc_L$, where c_S^i is the solid concentration at the interface and k is the partition coefficient.

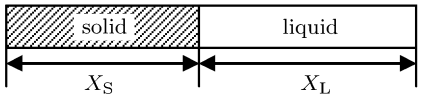


Fig.A1. Plate-like model of dendritic solidification.

The solute balance in the volume element can be written as follows:

$$\int_0^{X_S} c_S \mathrm{d}x + X_L c_L = X c_0, \tag{A1}$$

where c_0 is the initial liquid concentration, X_S and X_L are the lengths of the solid and liquid portions respectively, and $X = X_S + X_L$. Dividing through by X and writing the integral in term of the coordinate $\xi = x/X$, we find that this equation becomes:

$$\int_0^{f_S} c_S \mathrm{d}\xi + (1 - f_S)c_L = c_0. \tag{A2}$$

By differentiating with respect to time we obtain

$$\int_0^{f_S} \frac{\partial c_S}{\partial t}\mathrm{d}\xi + kc_L \frac{\mathrm{d}f_S}{\mathrm{d}t} - c_L \frac{\mathrm{d}f_S}{\mathrm{d}t} + (1 - f_S)\frac{\mathrm{d}c_L}{\mathrm{d}t} = 0. \tag{A3}$$

In the Scheil model the solid diffusion is neglected, which means $\dfrac{\partial c_S}{\partial t} = 0$, then Eq.(A3) reduces to:

$$c_L(1 - k)\mathrm{d}f_S = (1 - f_S)\mathrm{d}c_L. \tag{A4}$$

Integrating with the initial condition $c_L = c_x$ at $f_S = f_x$ (instead of $c_L = c_0$ at $f_S = 0$ in the case of standard microsegregation equation), we have

$$\frac{1}{1 - k}\int_{c_x}^{c_L} \frac{\mathrm{d}c_L}{c_L} = \int_{f_x}^{f_L} \frac{\mathrm{d}f_L}{f_L}, \tag{A5}$$

which results in

$$c_L = c_x \left(\frac{1 - f_S}{1 - f_x}\right)^{k-1}. \tag{A6}$$

This is the modified Scheil equation, which will reduce to standard form when $c_x = c_0$ and $f_x = 0$.

In the Lever rule the solid diffusion is complete and the solid concentration is uniform, so Eq.(A3) becomes

$$c_L(1 - k)\mathrm{d}f_S = (1 - f_S)\mathrm{d}c_L + kf_S\mathrm{d}c_L. \tag{A7}$$

Integrating with the initial condition $c_L = c_x$ at $f_S = f_x$, we can obtain

$$c_L = c_0 \frac{1 - (1 - k)f_x}{1 + (1 - k)f_S}, \tag{A8}$$

which will reduce to the standard lever rule when $c_x = c_0$ and $f_x = 0$.

For finite-rate diffusion in the solid Voller[4] proposed to set

$$\int_0^{f_S} \frac{\partial c_S}{\partial t} d\xi = \beta k f_S \frac{dc_L}{dt}, \tag{A9}$$

where β is the diffusion parameter. When β=2α, α is the Fourier number, Eq.(A3) can be written as:

$$c_L(1-k)df_S = (1-f_S)dc_L + 2\alpha k f_S dc_L. \tag{A10}$$

Integrating with the initial condition $c_L = c_x$ at $f_S = f_x$, we get in following result

$$c_L = c_x \left[\frac{1-(1-2\alpha k)f_S}{1-(1-2\alpha k)f_x}\right]^{\frac{k-1}{1-2\alpha k}}. \tag{A11}$$

In the limit of $c_x = c_0$ and $f_x = 0$, the standard Brody–Flemings equation

$$c_L = c_0[1-f_S(1-2\alpha k)]^{\frac{k-1}{1-2\alpha k}} \tag{A12}$$

follows immediately from Eq.(A11).

It can be seen that the modified Brody–Flemings equation (A11) will reduce to the modified Scheil equation (A6) with $\alpha = 0$, and reduce to the modified lever rule (A8) with $\alpha = 0.5$.

References

[1] Brody H D and Flemings M C 1966 *Trans. Metall. Soc. AIME* **236** 615
[2] Clyne T W and Kurz W 1981 *Metall. Trans.* A **12** 965
[3] Ohnaka I 1986 *Trans. ISIJ* **26** 1045
[4] Voller V R 1999 *J. Crystal Growth* **197** 325
[5] Giovanola B and Kurz W 1990 *Metall. Trans.* A **21** 260
[6] Voller V R and Beckermann C 1999 *Metall. Mater. Trans.* A **30** 2183
[7] Yan X, Xie F, Chu M and Chang Y A 2001 *Mater. Sci. Eng.* A **302** 268
[8] Warren J A and Boettinger W J 1995 *Acta Metall. Mater.* **43** 689
[9] Long W Y, Cai Q Z, Wei B K and Chen L L 2006 *Acta Phys. Sin.* **55** 1341 (in Chinese)
[10] Li M E, Xiao Z Y, Yang G C and Zhou Y H 2006 *Chin. Phys.* **15** 219
[11] Li J J, Wang J C, Xu Q and Yang G C 2007 *Acta Phys. Sin.* **56** 1514 (in Chinese)
[12] Kim S G, Kim W T and Suzuki T 1999 *Phys. Rev.* E **60** 7186
[13] Kobayashi R, Warren J A and Carter W C 2000 *Physica* D **140** 141
[14] Gránásy L, Pusztai T and Warren J A 2004 *J. Phys. Condens. Matter* **16** 1205
[15] Li J J, Wang J C, Xu Q and Yang G C 2007 *Acta Mater.* **55** 825
[16] Rappaz M and Gandin Ch A 1993 *Acta Metall. Mater.* **41** 345